

Pressure evolution of the low-temperature crystal structure and bonding of the superconductor FeSe ($T_c=37$ K)

S. Margadonna,^{1,*} Y. Takabayashi,² Y. Ohishi,³ Y. Mizuguchi,^{4,5,6} Y. Takano,^{4,5,6} T. Kagayama,⁷ T. Nakagawa,³ M. Takata,³ and K. Prassides^{2,†}

¹*School of Chemistry, University of Edinburgh, Edinburgh EH9 3JJ, United Kingdom*

²*Department of Chemistry, Durham University, Durham DH1 3LE, United Kingdom*

³*Japan Synchrotron Radiation Research Institute, SPring-8, Hyogo 679-5198, Japan*

⁴*National Institute for Materials Science, 1-2-1 Sengen, Tsukuba 305-0047, Japan*

⁵*TRIP, JST, 1-2-1 Sengen, Tsukuba 305-0047, Japan*

⁶*University of Tsukuba, 1-1-1 Tennodai, Tsukuba 305-0001, Japan*

⁷*Center for Quantum Science and Technology under Extreme Conditions, Osaka University, Osaka 560-8531, Japan*

(Received 13 March 2009; revised manuscript received 14 July 2009; published 11 August 2009)

α -FeSe with the PbO structure is a key member of the family of high- T_c iron pnictide and chalcogenide superconductors, as while it possesses the basic layered structural motif of edge-sharing distorted FeSe₄ tetrahedra, it lacks interleaved ion spacers or charge-reservoir layers. We find that the application of hydrostatic pressure first rapidly increases T_c which attains a broad maximum of 37 K at ~ 7 GPa before decreasing to 6 K upon further compression to ~ 14 GPa. Complementary synchrotron x-ray diffraction at 16 K was used to measure the low-temperature isothermal compressibility of α -FeSe, revealing an extremely soft solid with a bulk modulus, $K_0=30.7(1.1)$ GPa and strong bonding anisotropy between interlayer and intralayer directions that transforms to the more densely packed β polymorph above ~ 9 GPa. The nonmonotonic $T_c(P)$ behavior of FeSe coincides with drastic anomalies in the pressure evolution of the interlayer spacing, pointing to the key role of this structural feature in modulating the electronic properties.

DOI: [10.1103/PhysRevB.80.064506](https://doi.org/10.1103/PhysRevB.80.064506)

PACS number(s): 74.70.Dd, 61.05.C-, 74.25.Ha

I. INTRODUCTION

The α polymorph of the simple binary FeSe phase has recently emerged as a superconductor with an ambient P T_c of ~ 8 – 13 K.^{1,2} Its structure comprises stacks of edge-sharing FeSe₄ tetrahedra with a packing motif essentially identical to that of the FeAs layers in the families of the FeAs-based high- T_c superconductors^{3–7} but lacking any interleaved ion spacers or insulating layers. The structural analogy is reinforced by the observation that below 70 K the high-temperature crystal structure becomes orthorhombic (space group *Cmma*),⁸ displaying an identical distortion of the FeSe layers to that observed in the iron oxyarsenide family.^{9,10} Theoretical calculations also find a very similar two-dimensional electronic structure to that of the FeAs-based superconductors with cylindrical electron sections at the Brillouin-zone corner and cylindrical hole surface sections.¹¹ Moreover, superconductivity in FeSe is very sensitive to defects and disorder and occurs over a limited range of FeSe_{1- δ} nonstoichiometry.¹²

The effect of applied pressure on T_c provides crucial information to differentiate between competing models of superconductivity and in the FeSe binary, T_c is initially extremely sensitive to P and rises rapidly to 27 K at 1.48 GPa.² At the same time, antiferromagnetic spin fluctuations present above T_c are strongly enhanced by pressure.¹³ In the FeAs-based superconductors, the response of T_c to pressure is complex and sensitively depends on the composition of the materials and their doping level. Both positive and negative initial pressure coefficients, dT_c/dP have been measured. Typically for the REFeAsO_{1-x}F_x families, dT_c/dP is positive at low doping levels and switches over to a negative value as

x increases.^{14–18} Moreover, for systems where the initial dT_c/dP is positive, there is a critical value of P above which the trend is reversed and T_c decreases upon further pressurization.^{14,19}

Despite the importance of the evolution of T_c with P in understanding the superconducting properties of the Fe-based materials, there is currently little information on the detailed pressure dependence of their structural properties.^{20–22} Here we report on the conducting properties of FeSe as a function of P up to ~ 14 GPa; we find a very high initial pressure coefficient with T_c maximized at 37 K at ~ 7 GPa. At higher P , dT_c/dP becomes negative and T_c is reduced to 6 K at ~ 14 GPa. We also study the precise pressure evolution to 12.8 GPa of the FeSe structure at 16 K (i.e., well within the superconducting regime) by synchrotron x-ray powder diffraction. We find that the orthorhombic α polymorph survives to ~ 9 GPa whereupon the structure changes to that of the nonsuperconducting hexagonal β phase. T_c initially increases with P despite the decreasing SeFeSe thickness and the increasing distortion of the FeSe₄ units while the subsequent decrease clearly correlates with changes in the FeSe interlayer spacing.

II. EXPERIMENTAL DETAILS

The FeSe polycrystalline sample used in this work was prepared, as reported elsewhere.² High resolution synchrotron x-ray diffraction at ambient P is consistent with a stoichiometry Fe_{1.03}Se. Electrical resistivity measurements under high pressures were performed by a standard four-probe technique using a diamond-anvil cell (DAC). Powdered NaCl was used as pressure-transmitting medium. Pressure

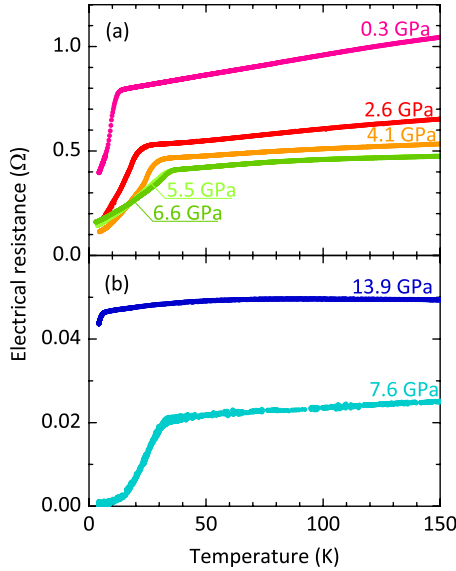


FIG. 1. (Color online) Resistance against temperature for FeSe at several applied pressures for (a) run 1 and (b) run 2.

was applied at room temperature and measured by the ruby fluorescence method. The measured values at low temperature are used to discuss the pressure dependence of T_c . The high-pressure synchrotron x-ray diffraction experiments at 16 K were performed at beamline BL10XU, SPring-8. The powder sample was loaded in a membrane DAC, which was placed inside a closed-cycle helium refrigerator. Daphne™ oil was used as a pressure medium. The applied pressure measured with the ruby fluorescence method was increased at 16 K without dismounting the cell from the cryostat. The diffraction patterns ($\lambda=0.41118$ Å) were collected using a flat image plate detector up to 12.8 GPa. Data analysis of the diffraction profiles was performed with the GSAS suite of Rietveld programs.

III. RESULTS

Figure 1(a) shows the temperature dependence of the resistance of the FeSe sample at various pressures. Superconductivity was observed below 13.4 K with a fairly sharp onset (run 1). T_c is found to increase initially rapidly upon the application of pressure with an accompanying increase in width and reaches a broad maximum of 37 K at 6.6 GPa—for binary solids, this high T_c is only surpassed by Cs_3C_{60} (38 K) (Ref. 23) and MgB_2 (39 K).²⁴ In a second experiment (run 2), P was increased first directly to 7.6 GPa and then to 13.9 GPa where the onset T_c is smaller at 6 K [Fig. 1(b)]. Pressure release to near ambient and subsequent pressurization to 9.7 GPa (run 3) resulted in smaller values of T_c —this may be related to the irreversibility of the $\alpha \rightarrow \beta$ structural transformation (*vide infra*) [Fig. 3(d)].

Inspection of the diffraction profile at 16 K and 0.25 GPa [Fig. 2(a)] readily reveals the orthorhombic (O) unit cell (space group $Cmma$) established for α -FeSe below 70 K at ambient P .⁸ Additional peaks are also evident and these can be accounted for by the presence of a minority hexagonal

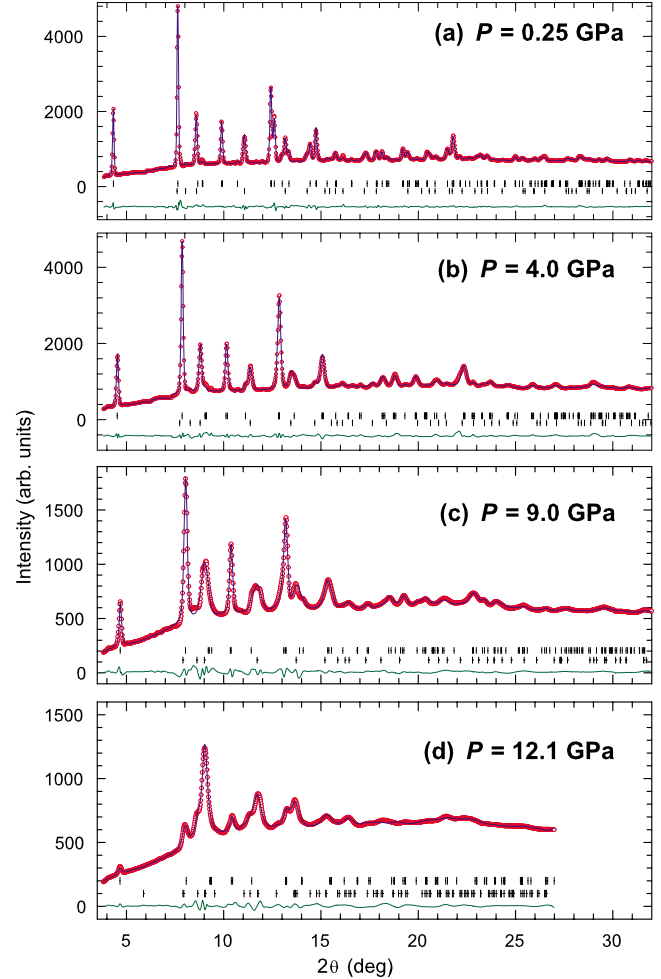


FIG. 2. (Color online) Final observed (red circles) and calculated (blue solid line) synchrotron x-ray ($\lambda=0.41118$ Å) powder-diffraction profiles at 16 K for the FeSe sample at (a) 0.25 GPa, (b) 4.0 GPa, (c) 9.0 GPa, and (d) 12.1 GPa. The lower green solid lines show the difference profiles and the tick marks show the reflection positions of the α - (upper) and β - (lower) phases, respectively. The diffraction profile collected at 12.1 GPa clearly shows the $\alpha \rightarrow \beta$ phase transformation. The β phase undergoes a phase transition from hexagonal to orthorhombic at 6.0 GPa.

NiAs-type β -FeSe phase [31.7(1)% fraction] (Table I). The diffraction data sets collected with increasing P show no structural changes for α -FeSe between 0.25 and 7.5 GPa with the α/β -phase assemblage remaining unaltered [Fig. 2(b)]. The same structural model was therefore employed in the Rietveld refinements in this pressure range, revealing a monotonic decrease in the lattice constants and unit-cell volume with increasing P [Figs. 3(a) and 3(b)]. However, the response of the lattice metrics to P is strongly anisotropic with the interlayer spacing showing a significantly larger contraction than the intralayer dimensions. As P increases, $2c/(a+b)$ smoothly decreases until at ~ 4 GPa, it approaches 1. Further increase in P leads to an even higher compression of the FeSe interlayer spacing [Fig. 3(c)] with $[2c/(a+b)]=0.987(2)$ at 7.5 GPa. However, as the sample is pressed to 9.0 GPa [Fig. 2(c)], the α -phase fraction begins to decrease and then it sharply collapses [inset of Fig. 2(b)]

TABLE I. Refined structural parameters and selected bond lengths (Å) and angles (°) for α -FeSe obtained from Rietveld refinements of synchrotron x-ray powder-diffraction data collected at 16 K with increasing pressure. Estimated errors in the last digits are given in parentheses.

Pressure	0.25 GPa	4.0 GPa	9.0 GPa	12.1 GPa
Temperature	16 K	16 K	16 K	16 K
α -FeSe				
Space group	<i>Cmma</i>	<i>Cmma</i>	<i>Cmma</i>	<i>Cmma</i> ^a
<i>a</i> (Å)	5.2952(10)	5.1749(13)	5.0835(12)	5.047(3)
<i>b</i> (Å)	5.3066(8)	5.2104(10)	5.1126(12)	5.085(4)
<i>c</i> (Å)	5.4545(3)	5.1943(8)	5.0304(9)	5.041(5)
Volume (Å ³)	153.27(1)	140.06(2)	130.74(2)	129.37(8)
Fraction (%)	68.3(1)	69.9(1)	64.7(1)	11.5(1)
Fe B_{iso} (Å ²)	0.96(7)	2.88(8)	1.0(1)	
Occ.	1.00	1.00	1.00	
Se <i>z</i>	0.2659(4)	0.2740(4)	0.2839(6)	
B_{iso} (Å ²)	2.40(6)	2.15(6)	1.51(8)	
Occ.	1.00	1.00	1.00	
Fe-Fe (Å)	2.6476(5) (×2)	2.5874(3) (×2)	2.5418(7) (×2)	
	2.6533(5) (×2)	2.6052(2) (×2)	2.5563(7) (×2)	
Fe-Se (Å)	2.370(1) (×4)	2.323(1) (×4)	2.300(1) (×4)	
Fe-Se-Fe (°)	104.53(9) (×2)	104.4(2) (×2)	103.2(1) (×2)	
	67.92(5) (×2)	67.69(5) (×2)	67.099(6) (×2)	
	68.09(5) (×2)	68.21(5) (×2)	67.53(6) (×2)	
Se-Se intraplane (Å)	3.7483(3) (×4)	3.6970(4) (×4)	3.6049(8) (×4)	
Se-Se interplane (Å)	3.679(3) (×2)	3.493(3) (×2)	3.345(4) (×2)	
β -FeSe				
Space group	<i>P6₃/mmc</i>	<i>P6₃/mmc</i>	<i>P6₃/mmc</i> ^b	<i>Pbnm</i> ^c
<i>a</i> (Å)	3.5904(2)	3.5090(6)	3.439(1)	5.896(1)
<i>b</i> (Å)				5.418(2)
<i>c</i> (Å)	5.8661(9)	5.684(2)	5.463(3)	3.4392(7)
Volume (Å ³)	65.489(9)	60.61(2)	55.95(2)	109.87(4)
Fraction (%)	31.7(1)	30.1(1)	35.3(1)	88.5(1)
R_{wp} (%)	3.09	2.49	2.62	3.89
R_{F^2} (%)	7.19	8.96	7.27	9.34

^aDue to the small phase fraction of the α -FeSe phase at 12.1 GPa, the Fe and Se fractional coordinates and isotropic temperature factors were not refined at this pressure.

^bThe evolution of the diffraction profiles clearly shows that the β -FeSe (NiAs-type) hexagonal phase begins to transform to the orthorhombic (MnP-type) phase above 6 GPa. However, the small phase fraction precluded accurate determination of the orthorhombic structural parameters and all refinements between 6 and 9 GPa were performed using the hexagonal cell to model the secondary β -FeSe phase.

^cIn the orthorhombic (MnP-type) phase, the Fe and Se atoms are positioned at [0.210(2), 0.063(1), 0.25] and [-0.107(1), 0.730(1), 0.25], respectively. Further work is needed to fully characterize the β -FeSe hexagonal-to-orthorhombic structural phase transition.

with an almost complete $\alpha \rightarrow \beta$ transformation taking place—at 12.1 GPa, the α -phase fraction is $\sim 12\%$ [Fig. 2(d)]. At the same time, while the basal plane lattice constants continue to contract, *c* begins to increase, resulting in saturation of the volume response to pressure and an increasing $2c/(a+b)$ ratio [Figs. 3(a)–3(c)]. Gradual depressurization to ~ 2 GPa does not lead to recovery of the orthorhombic α polymorph (its fraction remains at $\sim 12\%$), implying

that the $\alpha \rightarrow \beta$ phase transformation is irreversible at these low temperatures. Recovery of α -FeSe (53% fraction) at this *P* necessitated heating of the sample inside the DAC to 300 K.²⁵

Figure 3(b) shows the pressure evolution of the unit-cell volume of α -FeSe together with a least-squares fit of its 16 K equation of state to the semiempirical third-order Birch-Murnaghan equation.²⁶ The fit results in values of

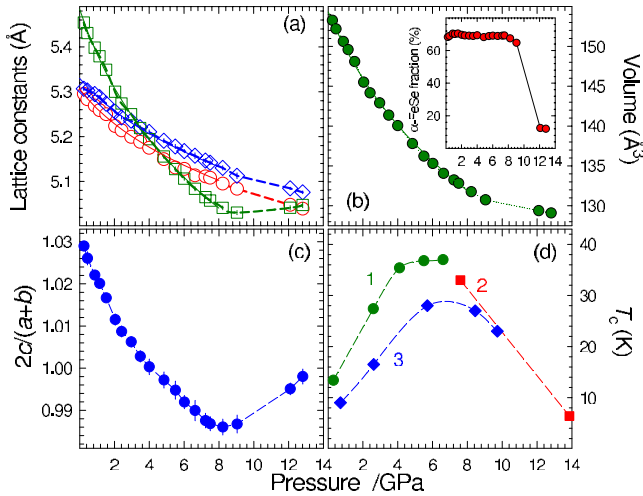


FIG. 3. (Color online) Pressure dependence of: (a) the orthorhombic lattice constants a (circles), b (diamonds), and c (squares), (b) the unit-cell volume, V , (c) the $[2c/(a+b)]$ ratio, and (d) the superconducting transition temperature, T_c (runs 1–3) of α -FeSe. The inset in (b) shows the pressure dependence of the α -FeSe phase fraction at 16 K. The solid lines through the data points to 7.5 GPa in (a) and (b) are least-squares fits to the Birch-Murnaghan equation of state while the dotted lines are guides to the eye.

the atmospheric pressure isothermal bulk modulus, $K_0 = 30.7(1.1)$ GPa and its pressure derivative, $K'_0 = 6.7(6)$ taking into account the $V(P)$ data to 7.5 GPa. The volume compressibility, $\kappa = d \ln V / dP = 0.033(1)$ GPa $^{-1}$ implies a soft highly compressible solid. A comparable value of the bulk modulus ~ 33 GPa at 50 K has been proposed from neutron-diffraction measurements over a restricted 0–0.6 GPa range.²⁷ The anisotropy in bonding of the α -FeSe structure [Fig. 4(d)] is clearly evident in Fig. 3(a) which displays the variation in the orthorhombic lattice constants with P . α -FeSe is least compressible in the basal plane in which the covalent Fe-Se bonds lie ($d \ln a / dP = 0.029(2)$ GPa $^{-1}$, $d \ln b / dP = 0.026(3)$ GPa $^{-1}$) while the interlayer compressibility, $d \ln c / dP = 0.065(4)$ GPa $^{-1}$ is ~ 2.5 times larger, implying very soft Se-Se interlayer interactions.

IV. DISCUSSION

The immediate consequence of the structural simplicity of FeSe is that the ~ 2.90 Å-thick SeFeSe building blocks are in close proximity separated from each other by only ~ 2.55 Å [Fig. 4(d)].⁸ This contrasts sharply with the enhanced interlayer separation in the FeAs analogs (e.g., inter-slab separation is ~ 5.79 Å in SmFeAsO which comprises interleaved SmO layers²⁸ and ~ 3.45 and 3.34 Å in SrFe₂As₂ and LiFeAs which possess Sr²⁺ and Li⁺ spacers, respectively).^{5,6} As a result, the c axis in FeSe is only marginally larger (1.03 times) than the average basal plane dimensions. The electronic consequence of this structural size proximity should be to render the electronic structure of FeSe more three dimensional in nature than those of any of the related FeAs superconductors. Moreover, given the soft-

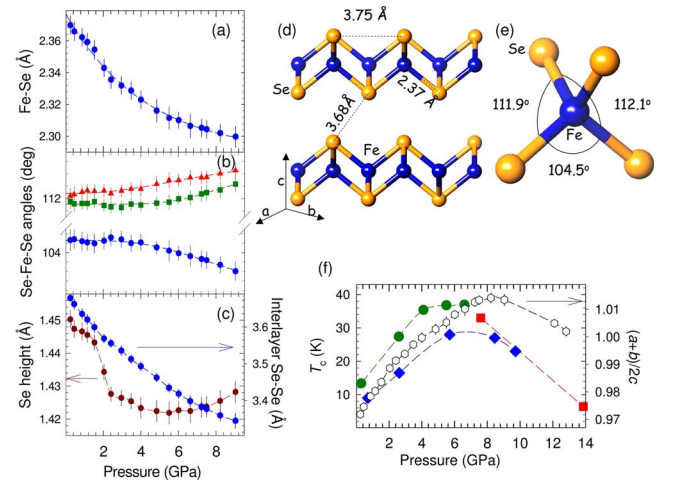


FIG. 4. (Color online) [(a)–(c)] Pressure dependence of: (a) the Fe-Se bond distances, (b) the three distinct Se-Fe-Se bond angles, and (c) the interlayer Se-Se contacts and the height of the Se atoms above the Fe plane for the orthorhombic crystal structure of α -FeSe at 16 K. (d) Schematic diagram of the crystal structure of α -FeSe with selected distances at 16 K and 0.25 GPa. (e) Geometry of the FeSe₄ units and definition of the three Se-Fe-Se bond angles together with their values at 16 K and 0.25 GPa. (f) Pressure dependence of the $[(a+b)/2c]$ ratio at 16 K and the superconducting T_c of α -FeSe. The lines through the points are guides to the eye.

ness of the interlayer Se-Se interactions relative to the covalently bonded SeFeSe slabs, the application of pressure should have a profound influence on the structural and electronic dimensionalities, allowing their tuning at interlayer contact separations inaccessible in other currently known Fe-based superconductors. This is of key importance if we recall both the extreme sensitivity of T_c to P and its nonmonotonic response at high P . The distinct structural response to P of α -FeSe is clearly apparent by considering the compressibility and its anisotropy [Figs. 3(a) and 3(b)]. Firstly, the low- T bulk modulus, $K_0 = 30.7(1.1)$ GPa is the smallest measured thus far in any of these systems— K_0 is 57.3(6) GPa for LiFeAs,²² 78(2) GPa for LaFeAsO_{0.9}F_{0.1}, and 102(2) GPa for NdFeAsO_{0.88}F_{0.12}.^{20,21} In addition, the compressibility of α -FeSe along the interlayer direction is the largest among these systems—the c axis contracts by 7.3% at 7.5 GPa—while the basal plane compressibility (contraction by 3.3% at 7.5 GPa) is comparable to that in LiFeAs but considerably larger than those of the iron oxyarsenides.

This sets the scene to discuss the pressure response of T_c in α -FeSe and its relationship to the structural evolution with P . Figures 4(a) and 4(c) show the pressure dependence at 16 K of the Fe-Se and Se-Se interatomic distances. The Fe-Se bonds contract smoothly with an overall decrease of 2.9% at 9.0 GPa. Similarly the intralayer Se-Se distances decrease monotonically with a somewhat larger contraction of 3.8%. However, the pressure response of the interlayer Se-Se contacts is much steeper with a 9.1% decrease reflecting the very large interlayer compressibility—the SeFeSe slabs approach each other rapidly up to 7.5 GPa but then their contact distance appears to saturate. As a result, there is a correlation between the pressure evolution of the unit-cell metrics and

the superconducting T_c [Fig. 4(f)]. At low pressures, the rapid increase in $(a+b)/2c$ is mirrored by the rapidly increasing T_c (α -FeSe has the smallest bulk modulus and highest pressure coefficient of T_c among the Fe-based superconductors). Remarkably the pressure range at which the maximum T_c is found coincides with the onset of the structural anomalies. While the basal plane lattice constants continue to contract smoothly, the interlayer spacing begins to expand slightly leading to a decreasing $(a+b)/2c$ ratio as P increases above 7.5 GPa. Thus it is tempting to ascribe the nonmonotonic $T_c(P)$ behavior to the competition between the effects of the interlayer SeSe interactions (tuning the doping level) and the intralayer FeSe bonding and suggests that higher T_c 's are associated with smaller interlayer spacings (increased dimensionality).

Figures 4(b) and 4(c) show the pressure dependence at 16 K of the thickness of the SeFeSe slabs and the crystallographic bond angles of the FeSe₄ tetrahedra [Fig. 4(e)]. It has been argued for the iron (oxy)arsenides that the geometry of the edge-sharing FeAs₄ tetrahedral units sensitively controls the width of the electronic conduction band and therefore the magnitudes of the slab thickness and the As-Fe-As angles are important parameters in tuning the electronic properties of these systems and determining T_c .^{29–31} Empirically T_c appears to be maximal when the FeAs₄ units are close to regular with As-Fe-As angles of 109.47°. Along these lines, the observation of negative pressure coefficients of T_c has been rationalized in terms of increased tetrahedral distortion away from regular shape.^{21,22,32} α -FeSe has an identical distortion mode of the FeSe₄ tetrahedra with a sizable distortion away from regularity [7.5° angle difference, Fig. 4(e)]. However, while the distortion also increases significantly with increasing P and the SeFeSe slab thickness decreases [Figs. 4(b) and 4(c)], the pressure coefficient of T_c is positive in this range, implying that the empirical generalization which appears to hold well for the iron (oxy)arsenides is not applicable in the present system—apparently the dependence of the electronic structure on the interlayer separation dominates in determining the superconducting properties of α -FeSe.

Finally, we discuss the high- P $\alpha \rightarrow \beta$ transformation. First, pressurization leads to a rapid decrease in the α -phase

Se-Se interlayer contacts, which approach a value of 3.3 Å at 7.5 GPa. As a result, the sign of the compressibility along c changes and the interlayer spacing begins to increase upon further increase in P . In addition, the three-dimensional β -FeSe is more densely packed than the quasi-two-dimensional α polymorph. The large difference in packing density is retained at high P and at 9.0 GPa, the $\alpha \rightarrow \beta$ transition is accompanied by a $\sim 15.1\%$ decrease in volume as the Fe-Se coordination changes from tetrahedral to the more densely packed octahedral one. At the same time, the transition results in an increase in the Fe-Fe and Fe-Se distances by 7.4% and 4.9%, respectively. These observations point toward a scenario where the α phase cannot sustain pressures above 9 GPa as the interlayer separation is now so small that it is energetically favorable to form the more efficiently packed β phase with a release of the bonding distances.

Recently, a paper appeared with partially overlapping results on the pressure dependence of T_c (which is found to reach a maximum of 36.7 K at 8.9 GPa) and the stability of the α -FeSe phase (which transforms to the nonsuperconducting hexagonal NiAs-type phase above 7 GPa at ambient temperature) that are in excellent agreement to those presented here.³³

V. CONCLUSION

In conclusion, we have found that the superconductivity onset in α -FeSe attains a broad maximum of 37 K at ~ 7 GPa. The orthorhombically distorted superconducting phase is extremely soft and the pressure response of the structure reveals an intimate link between the SeFeSe interlayer separations and the superconducting properties. Detailed band-structure calculations should be able to shed light on the accompanying evolution of the doping level of the SeFeSe layers and decipher the relative importance between the increased dimensionality and the FeSe slab geometry to superconductivity.

ACKNOWLEDGMENTS

We thank SPring-8 for access to the synchrotron x-ray facilities and K. Kuroki for useful discussions.

*serena.margadonna@ed.ac.uk

†k.prassides@durham.ac.uk

¹F.-C. Hsu, J.-Y. Luo, K.-W. Yeh, T.-K. Chen, T.-W. Huang, P. M. Wu, Y.-C. Lee, Y.-L. Huang, Y.-Y. Chu, D.-C. Yan, and M.-K. Wu, Proc. Natl. Acad. Sci. U.S.A. **105**, 14262 (2008).

²Y. Mizuguchi, F. Tomioka, S. Tsuda, T. Yamaguchi, and Y. Takano, Appl. Phys. Lett. **93**, 152505 (2008).

³Y. Kamihara, T. Watanabe, M. Hirano, and H. Hosono, J. Am. Chem. Soc. **130**, 3296 (2008).

⁴X. H. Chen, T. Wu, G. Wu, R. H. Liu, H. Chen, and D. F. Fang, Nature (London) **453**, 761 (2008).

⁵M. Rotter, M. Tegel, and D. Johrendt, Phys. Rev. Lett. **101**, 107006 (2008).

⁶M. J. Pitcher, D. R. Parker, P. Adamson, S. J. C. Herkelrath, A. T. Boothroyd, R. M. Ibberson, M. Brunelli, and S. J. Clarke, Chem. Commun. (Cambridge) **2008**, 5918.

⁷J. H. Tapp, Z. Tang, B. Lv, K. Sasmal, B. Lorenz, P. C. W. Chu, and A. M. Guloy, Phys. Rev. B **78**, 060505(R) (2008).

⁸S. Margadonna, Y. Takabayashi, M. T. McDonald, K. Kasperkiewicz, Y. Mizuguchi, Y. Takano, A. N. Fitch, E. Suard, and K. Prassides, Chem. Commun. (Cambridge) **2008**, 5607.

⁹C. de la Cruz, Q. Huang, J. W. Lynn, J. Li, W. Ratcliff, J. L. Zarestky, H. A. Mook, G. F. Chen, J. L. Luo, N. L. Wang, and P. Dai, Nature (London) **453**, 899 (2008).

¹⁰T. Nomura, S. W. Kim, Y. Kamihara, M. Hirano, P. V. Sushko, K. Kato, M. Takata, A. L. Shluger, and H. Hosono, Supercond. Sci.

- Technol. **21**, 125028 (2008).
- ¹¹A. Subedi, L. Zhang, D. J. Singh, and M.-H. Du, Phys. Rev. B **78**, 134514 (2008).
- ¹²T. M. McQueen, Q. Huang, V. Ksenofontov, C. Felser, Q. Xu, H. W. Zandbergen, Y. S. Hor, J. Allred, A. J. Williams, D. Qu, J. Checkelsky, N. P. Ong, and R. J. Cava, Phys. Rev. B **79**, 014522 (2009).
- ¹³T. Imai, K. Ahilan, F. L. Ning, T. M. McQueen, and R. J. Cava, Phys. Rev. Lett. **102**, 177005 (2009).
- ¹⁴H. Takahashi, K. Igawa, K. Arii, Y. Kamihara, M. Hirano, and H. Hosono, Nature (London) **453**, 376 (2008).
- ¹⁵Y. Takabayashi, M. T. McDonald, D. Papanikolaou, S. Margadonna, G. Wu, R. H. Liu, X. H. Chen, and K. Prassides, J. Am. Chem. Soc. **130**, 9242 (2008).
- ¹⁶B. Lorenz, K. Sasmal, R. P. Chaudhury, X. H. Chen, R. H. Liu, T. Wu, and C. W. Chu, Phys. Rev. B **78**, 012505 (2008).
- ¹⁷N. Takeshita, A. Iyo, H. Eisaki, H. Kito, and T. Ito, J. Phys. Soc. Jpn. **77**, 075003 (2008).
- ¹⁸W. Yi, L. Sun, Z. Ren, W. Lu, X. Dong, H.-J. Zhang, X. Dai, Z. Fang, Z. Li, G. Che, J. Yang, X. Shen, F. Zhou, and Z. Zhao, EPL **83**, 57002 (2008).
- ¹⁹P. L. Alireza, Y. T. C. Ko, J. Gillett, C. M. Petrone, J. M. Cole, G. G. Lonzarich, and S. E. Sebastian, J. Phys.: Condens. Matter **21**, 012208 (2009).
- ²⁰G. Garbarino, P. Toulemonde, M. Álvarez-Murga, A. Sow, M. Mezouar, and M. Núñez-Regueiro, Phys. Rev. B **78**, 100507(R) (2008).
- ²¹J. Zhao, L. Wang, D. Dong, Z. Liu, H. Liu, G. Chen, D. Wu, J. Luo, N. Wang, Y. Yu, C. Jin, and Q. Guo, J. Am. Chem. Soc. **130**, 13828 (2008).
- ²²M. Mito, M. J. Pitcher, W. Crichton, G. Garbarino, P. J. Baker, S. J. Blundell, P. Adamson, D. R. Parker, and S. J. Clarke, J. Am. Chem. Soc. **131**, 2986 (2009).
- ²³A. Y. Ganin, Y. Takabayashi, Y. Z. Khimyak, S. Margadonna, A. Tamai, M. J. Rosseinsky, and K. Prassides, Nature Mater. **7**, 367 (2008).
- ²⁴J. Nagamatsu, N. Nakagawa, T. Muranaka, Y. Zenitani, and J. Akimitsu, Nature (London) **410**, 63 (2001).
- ²⁵ β -FeSe undergoes a phase transition to a lower symmetry structure at 16 K and 6.0 GPa. The observed Bragg reflections are well accounted for by a MnP-type orthorhombic structure (space group $Pbnm$) with lattice constants related to those of the low-pressure NiAs-type hexagonal unit cell (space group $P6_3/mmc$) by $a_o = \sqrt{3}a_h$, $b_o = c_h$, and $c_o = a_h$.
- ²⁶R. J. Angel, Rev. Mineral. Geochem. **41**, 35 (2000).
- ²⁷J. N. Millican, D. Phelan, E. L. Thomas, J. B. Leao, and E. Carpenter, Solid State Commun. **149**, 707 (2009).
- ²⁸S. Margadonna, Y. Takabayashi, M. T. McDonald, M. Brunelli, G. Wu, R. H. Liu, X. H. Chen, and K. Prassides, Phys. Rev. B **79**, 014503 (2009).
- ²⁹J. Zhao, Q. Huang, C. de la Cruz, S. Li, J. W. Lynn, Y. Chen, M. A. Green, G. F. Chen, G. Li, Z. Li, J. L. Luo, N. L. Wang, and P. Dai, Nature Mater. **7**, 953 (2008).
- ³⁰T. M. McQueen, M. Regulacio, A. J. Williams, Q. Huang, J. W. Lynn, Y. S. Hor, D. V. West, M. A. Green, and R. J. Cava, Phys. Rev. B **78**, 024521 (2008).
- ³¹C.-H. Lee, A. Iyo, H. Eisaki, H. Kito, M. T. Fernandez-Diaz, T. Ito, K. Kihou, H. Matsuhata, M. Braden, and K. Yamada, J. Phys. Soc. Jpn. **77**, 083704 (2008).
- ³²R. Kumai, N. Takeshita, T. Ito, H. Kito, A. Iyo, and H. Eisaki, J. Phys. Soc. Jpn. **78**, 013705 (2008).
- ³³S. Medvedev, T. M. McQueen, I. A. Troyan, T. Palasyuk, M. I. Erements, R. J. Cava, S. Naghavi, F. Casper, V. Ksenofontov, G. Wortmann, and C. Felser, Nature Mater. **8**, 630 (2009).